



HAL
open science

Gravity and magnetic data inversion for 3D topography of the Moho discontinuity in the northern Red Sea area, Egypt

Ilya Prutkin, Ahmed Saleh

► **To cite this version:**

Ilya Prutkin, Ahmed Saleh. Gravity and magnetic data inversion for 3D topography of the Moho discontinuity in the northern Red Sea area, Egypt. *Journal of Geodynamics*, 2009, 47 (5), pp.237. 10.1016/j.jog.2008.12.001 . hal-00531896

HAL Id: hal-00531896

<https://hal.science/hal-00531896>

Submitted on 4 Nov 2010

HAL is a multi-disciplinary open access archive for the deposit and dissemination of scientific research documents, whether they are published or not. The documents may come from teaching and research institutions in France or abroad, or from public or private research centers.

L'archive ouverte pluridisciplinaire **HAL**, est destinée au dépôt et à la diffusion de documents scientifiques de niveau recherche, publiés ou non, émanant des établissements d'enseignement et de recherche français ou étrangers, des laboratoires publics ou privés.

Accepted Manuscript

Title: Gravity and magnetic data inversion for 3D topography of the Moho discontinuity in the northern Red Sea area, Egypt

Authors: Ilya Prutkin, Ahmed Saleh

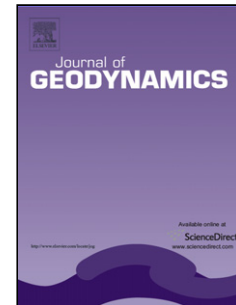
PII: S0264-3707(08)00091-4
DOI: doi:10.1016/j.jog.2008.12.001
Reference: GEOD 871

To appear in: *Journal of Geodynamics*

Received date: 2-9-2008
Revised date: 28-11-2008
Accepted date: 5-12-2008

Please cite this article as: Prutkin, I., Saleh, A., Gravity and magnetic data inversion for 3D topography of the Moho discontinuity in the northern Red Sea area, Egypt, *Journal of Geodynamics* (2008), doi:10.1016/j.jog.2008.12.001

This is a PDF file of an unedited manuscript that has been accepted for publication. As a service to our customers we are providing this early version of the manuscript. The manuscript will undergo copyediting, typesetting, and review of the resulting proof before it is published in its final form. Please note that during the production process errors may be discovered which could affect the content, and all legal disclaimers that apply to the journal pertain.



Gravity and magnetic data inversion for 3D topography of the Moho discontinuity in the northern Red Sea area, Egypt

Ilya Prutkin ^{a,*}, Ahmed Saleh ^b

^a*Delft University of Technology, Netherlands*

^b*National Research Institute of Astronomy and Geophysics, Helwan, Cairo, Egypt*

Abstract

The main goal of our study is to investigate 3D topography of the Moho boundary for the area of the northern Red Sea including Gulf of Suez and Gulf of Aqaba. For potential field data inversion we apply a new method of local corrections. The method is efficient and does not require trial-and-error forward modeling. To separate sources of gravity and magnetic field in depth, a method is suggested, based on upward and downward continuation. Both new methods are applied to isolate the contribution of the Moho interface to the total field and to find its 3D topography. At the first stage, we separate near-surface and deeper sources. According to the obtained field of shallow sources a model of the horizontal layer above the depth of 7 km is suggested, which includes a density interface between light sediments and crystalline basement. Its depressions and uplifts correspond to known geological structures. At the next stage, we isolate the effect of very deep sources (below 100 km) and sources outside the area of investigation. After subtracting this field from the total effect of deeper sources, we obtain the contribution of the Moho interface. We make inversion separately for the area of rifts (Red Sea, Gulf of Suez and Gulf of Aqaba) and for the rest of the area. In the rift area we look for the upper boundary of low-density, heated anomalous upper mantle. In the rest of the area the field is satisfied by means of topography for the interface between lower crust and normal upper mantle. Both algorithms are applied also to the magnetic field. The magnetic model of the Moho boundary is in agreement with the gravitational one.

Key words: 3D gravity and magnetic data inversion, Moho boundary, Computational methods: potential fields, Contact surface topography, Northern Red Sea

* Corresponding author. Tel.: +31 1527 87394; Fax: +31 1527 82348.
Email address: I.Prutkin@tudelft.nl (Ilya Prutkin).

1 Introduction

The Red Sea is considered to be a typical example of a newly formed ocean. Therefore, since the discovery of plate tectonics, a great number of studies discussed its evolution as a key to the understanding of continental rifting and the initiation of sea floor spreading (Drake and Girdler, 1964; Tramontini and Davies, 1969; Makris et al., 1983; Gaulier et al., 1988; Meshref, 1990). The northern part of the Red Sea appears to be characterized by oceanic type crust, lying at a mean depth of 7 to 8 km, whereas the Moho is at a mean depth of 10 to 13 km, and at 32 km closest to the coastline (Gaulier et al., 1988; Makris et al., 1991; Rihm et al., 1991). In the Gulf of Suez, the top of the crust is at a depth of 5 km. The Moho is found at a relatively shallow depth of 18 to 20 km and at a mean depth of 30 to 35 km both under southern Sinai and Eastern Desert plateaus (Gaulier et al., 1988; Saleh et al., 2006). Refraction data indicate the Moho depth of 35 to 40 km in the areas not affected by the rifting event (Ginzburg et al., 1981; Makris et al., 1983; Gettings et al., 1986; El-Isa et al., 1987). The anomalous nature of the upper mantle (8.0 km/s) and the thinning of the crust beneath the northern Red Sea rift are well known from the results of seismic and gravity studies. The density values of the different geological sedimentary units and the megastructures (the crust and the upper mantle) of the present study are based on the P-wave velocity distribution in the northern Red Sea and the Gulf of Suez (Gaulier et al., 1988).

Our goal is to retrieve the 3D geometry of the Moho interface for the northern Red Sea area by means of two new algorithms for gravity and magnetic data inversion and for separating sources in depth. Till now the usual approach to find 3D topography of a contact surface is forward gravity modeling. One changes an initial model in interactive way to diminish gravity residuals. Recently this approach has been applied, for instance, to study a geological structure of the northern Red Sea area in Saleh et al. (2006) using the package IGMAS (Götze and Lahmeyer, 1988) for interactive gravity modeling. The disadvantages of the forward modeling approach are following. One changes the model of the geological section from one profile to another, but changes in one vertical section influence the gravity field along other profiles. Each section takes into account a lot of geological and seismic a priori information, but the number of parameters, per section, is much larger, than the number of profile observations, it is not reasonable from the viewpoint of stability. The problems of non-uniqueness and instability of gravity data inversion are not likely to be solved by a forward modeling approach.

A different approach is applied by Tirel et al. (2004) to obtain the Moho topography to the north of Crete, the linearized inverse problem is solved by means of the Fourier Transform (Parker, 1972; Oldenburg, 1974). In our inves-

tigation we use quite a different procedure. We solve an integral equation for a function determining geometry of an unknown contact surface. The kernel of this equation, evaluating the gravitational effect of a contact surface, depends in a nonlinear way on the sought function. The 3D inverse problem is solved in a full (nonlinear) statement by means of the method of local corrections (Prutkin, 1983, 1986) without any linearization. This method does not make use of nonlinear minimization, which reduces the computer calculation time by an order of magnitude. The local corrections method takes the non-uniqueness and instability of the inverse problem into account.

Our method of inversion is of the same type, as the method of Cordell and Henderson (1968). A solution is calculated from gravity data automatically by successive approximations, without a time-consuming trial-and-error process. Like in the algorithm of Cordell and Henderson (1968), density contrast and the position of a horizontal reference plane should be specified to obtain a unique solution. We apply a different approach to form a successive approximation. Moreover, we take into account instability of the inverse problem by means of a sort of regularization. We have mentioned only a few different approaches for gravity data inversion. A detailed overview of the literature on the potential field inverse problem can be found in Blakely (1995). In the algorithm of Cordell and Henderson (1968) density contrast is assumed to be uniform. In our approach it can be different in every point; an elementary column is not homogeneous in the vertical direction above and below the unknown contact surface; moreover, we apply the method of local corrections both for gravity and magnetic data inversion.

The paper is organized as follows: we present new mathematical algorithms for isolating sources in depth and for 3D gravity and magnetic data inversion, and then both algorithms are applied to the northern Red Sea area to extract the effect of the Moho interface and to find its 3D topography. We start with our mathematical theory; it is presented in the first section. As a preliminary pre-processing of gravity and magnetic observations, the new algorithm is suggested to extract the effect of the contact surface sought. The main idea of the algorithm is to eliminate sources from the Earth's surface up to a prescribed depth by means of upward and downward continuation. In the same section 2, the method of local corrections applied to a 3D contact surface topography recovery is described. Next, we start with application of our algorithms for the northern Red Sea area. In section 3 we separate sources of the gravitational field into shallow and deeper ones and construct a model of the near-surface layer. Then we isolate the gravitational effect of the Moho interface and find its 3D topography. In section 4 we make the same based on magnetic data. Section 5 contains the main conclusions of our study.

2 Mathematical theory

The main purpose of the algorithm to separate sources in depth is to find the part of the observed field, which is harmonic above a given depth h . We can treat this function as an effect of the half-space below the depth h . To find such a function means to eliminate all sources located in the horizontal layer from the Earth surface up to a prescribed depth. The algorithm allows to separate the effects of shallow and deeper objects and to extract the gravity signal of sources located in horizontal layer between given depths h_1 and h_2 .

The algorithm is based on upward and downward continuation (Vasin, Prutkin and Timerkhanova, 1996; Martyshko and Prutkin, 2003). There are two problems to be solved. Firstly, we continue the data upward to the height h to diminish the influence of the sources in the near-surface layer. This operation causes the main errors in the vicinity of the boundary of the area. To reduce them we need some model of the regional field to subtract it from the observed field prior to upward continuation. Secondly, we continue the obtained function downward to the depth h , i.e. to the distance $2h$ in downward direction. The problem of downward continuation is a linear ill-posed inverse problem, therefore we must use some regularization.

The function, which we treat as a regional field, is assumed to be harmonic in the area (in two-dimensional sense) and to have the same values at the boundary of the area, as the observed field:

$$\begin{cases} \Delta_2 f = \frac{\partial^2 f}{\partial x^2} + \frac{\partial^2 f}{\partial y^2} = 0 & \text{within area } S \\ f = \Delta g & \text{on its boundary } \partial S \end{cases} \quad (1)$$

If we subtract the values of this function, the residual field will be equal to zero at the boundary of the area, therefore no errors are introduced, when we integrate the residual field while upward continuation along the restricted area. According to the properties of harmonic functions, this function has no extremum within the area, so we create no false anomalies. Besides, as it is known from calculus of variations (Gelfand and Fomin, 2000), a solution of the problem (1) provides a minimum of the following functional:

$$J(f) = \iint_S \left(\left(\frac{\partial f}{\partial x} \right)^2 + \left(\frac{\partial f}{\partial y} \right)^2 \right) dx dy \longrightarrow \min, \quad (2)$$

therefore, we obtain the smoothest possible function with given values on the boundary. All these properties allow us to regard this function as a model of the regional field.

After subtracting the suggested model of the regional field we make upward continuation of the residual field by means of the following formula:

$$\frac{1}{2\pi} \iint \frac{h}{((x-x')^2 + (y-y')^2 + h^2)^{3/2}} U(x, y, 0) dx dy = U(x', y', h) \quad (3)$$

The formula (3) gives a solution of the Dirichlet problem: to find a harmonic function in the upper half-space with given values on the boundary (on the plane $z = 0$).

At the second step we continue the obtained function downward to the depth h , i.e. to the distance $2h$ in downward direction. To do this, we apply a formula similar to (3):

$$\frac{1}{2\pi} \iint \frac{h_1}{((x-x')^2 + (y-y')^2 + h_1^2)^{3/2}} U(x, y, -h) dx dy = U(x', y', h) \quad , \quad (4)$$

where $h_1 = 2h$. Formula (4) provides a function, which is harmonic in a half-space above the plane $z = -h$. But this time we treat the formula as an integral equation: the right hand is given, and we have to find the unknown function $U(x, y, -h)$.

Although the influence of shallow sources is diminished after upward continuation, the rest of them is still presented in the field, so we make downward continuation *through* the sources. It should be emphasized, that the problem of downward continuation is a linear ill-posed inverse problem, therefore we must use some regularization. Since the integral operator A in (4) is self-adjoint and positive, we apply the Lavrent'ev's approach (Lavrent'ev et al., 1986). If we write (4) in the following form: $Au = u_h$, u is an unknown field on the level $z = -h$, u_h is the obtained field on the height h , then the Lavrent'ev's regularization gives: $(A + \alpha I)u = u_h$, where I is identity operator, α – a regularizing parameter. Therefore, after discretization no matrix multiplication is required.

At last we calculate the field on the Earth's surface $z = 0$ using a formula, similar to (3). We obtain a part of the field, which is harmonic up to the depth h , so we could treat it as an effect from the deeper sources.

To evaluate the gravitational effect of a contact surface, we consider a following model of a two-layer gravitational medium in 3D space. The model consists of two layers of a constant density σ_1 and σ_2 , separated by the surface S . Suppose that, in the Cartesian coordinate system, the plane xOy coincides with the Earth surface, and the axis z is directed downward. The upper layer

is bounded above by the horizontal plane $z = h_-$, $h_- \geq 0$, and below by the surface S ; the lower layer is bounded above by the surface S and below by the plane $z = h_+$; at $z < h_-$ and $z > h_+$ masses are absent. The unknown contact surface is determined by the equation $z = z(x, y)$. It is assumed that $z(x, y)$ is a single-valued limited function, and that for a certain H

$$\lim_{\substack{|x| \rightarrow \infty \\ |y| \rightarrow \infty}} |z(x, y) - H| = 0, \quad (5)$$

i.e., the surface S has a horizontal asymptotic plane $z = H$. If we subtract the effects of two Bouguer plates, we find, that the field of our two-layer model accurate to a constant term is the field of masses contained between the surface S and the plane $z = H$, with a density $\pm \Delta\sigma$, where $\Delta\sigma = \sigma_2 - \sigma_1$ is the density contrast at the contact surface. The field of such an object is evaluated by the formula

$$\Delta g(x', y', 0) = G \Delta\sigma \int_{-\infty}^{\infty} \int_{-\infty}^{\infty} \left(\frac{1}{\sqrt{(x-x')^2 + (y-y')^2 + z^2(x, y)}} - \frac{1}{\sqrt{(x-x')^2 + (y-y')^2 + H^2}} \right) dx dy, \quad (6)$$

where G is the gravitational constant. We can regard formula (6) as a nonlinear integral equation of the 1st kind with respect to the unknown function $z(x, y)$. Suppose that the field at the Earth surface is given on a rectangular grid $\{x_i, y_j\}$. We divide a volume between the surface S and the plane $z = H$ into a number of elementary prisms, for each prism the projection of its center onto the plane xOy coincides with some observation point. The mean heights of the prisms are taken as unknown parameters. Their number equals exactly to the number of observations N . Denote by $K(x', y', x, y, z(x, y))$ the integrand in (6). This expression was referred in (Snopek and Casten, 2006) as the gravity attraction of a linear, vertical mass. It has been suggested there to apply it as an approximation of the exact formula for the prism gravity. It means, that while discretizing (6) by numerical integration we use one-point cubature formula for each elementary prism, which gives

$$c G \Delta\sigma \sum_i \sum_j K_{i_0 j_0}(z_{ij}) = U_{i_0 j_0}, \quad (7)$$

where c is the weight of the cubature formula, $z_{ij} = z(x_i, y_j)$, and

$$U_{i_0j_0} = \Delta g(x_{i_0}, y_{j_0}, 0), K_{i_0j_0}(z_{ij}) = K(x_{i_0}, y_{j_0}, x_i, y_j, z_{ij}).$$

To increase the accuracy one could apply for discretisation (6) Gauss cubature, in this case each term in (7) will be substituted by several similar ones, corresponding to the same z_{ij} .

Our goal is to develop an iterative procedure for solving the system of non-linear equations (7). Suppose that z_{ij}^n are the values of the unknown function obtained at the n -th step. For the corresponding solution of the direct problem we introduce the notation

$$U_{i_0j_0}^n = c G \Delta \sigma \sum_i \sum_j K_{i_0j_0}(z_{ij}^n). \quad (8)$$

The method of local corrections is based on the fact that the variation of the field at a certain point is affected mostly by the variation of the part of the object boundary closest to this point. At each step we try to reduce the difference between the given and the approximate values of the field at a given node solely by modifying the value of the unknown function at that node. If the value of the unknown function in one point only has been changed, then the sum in (8) for the next iteration differs only in one term. Assuming that in the chosen node $U_{ij}^{n+1} = U_{ij}$ and subtracting (8) from the similar equality corresponding to the $(n+1)$ -th step, we obtain the fundamental equation to find the next approximation (Prutkin, 1986):

$$G \Delta \sigma \left(K_{ij}(z_{ij}^{n+1}) - K_{ij}(z_{ij}^n) \right) = \alpha \left(U_{ij} - U_{ij}^n \right). \quad (9)$$

The coefficient α in the right hand of (9) is introduced to slow down the change of the model.

It turns out that, in the case of a contact surface, Eq. (9) can be converted to a very simple form. Indeed, considering Eq. (6), we have

$$K_{ij}(z_{ij}^n) = 1/z_{ij}^n - 1/H \quad (10)$$

Using (10), we rewrite Eq. (9) as

$$G \Delta \sigma \left(1/z_{ij}^{n+1} - 1/z_{ij}^n \right) = \alpha \left(U_{ij} - U_{ij}^n \right)$$

and finally

$$z_{ij}^{n+1} = \frac{z_{ij}^n}{1 + \alpha s z_{ij}^n (U_{ij} - U_{ij}^n)} \quad , \quad (11)$$

where $s = (G\Delta\sigma)^{-1}$. According to (11), several arithmetic operations are sufficient to obtain the next successive approximation at each point of the grid. We have to store only the vector of unknowns of the same length N as the length of the observations vector. The full (nonlinear) inverse problem is solved without any linearization, and we don't need to store some matrix of the size $N \times N$.

It is known, that for the fixed values of the density contrast $\Delta\sigma$ and the depth to the asymptotic plane H , a solution of the inverse problem for a contact surface is unique. In the same time, taking different values of these parameters, one could obtain different solutions causing the same gravity field. In (Prutkin, 1986), a family of contact surfaces is presented, which generate with different values of $\Delta\sigma$ and H the same field, as a point source.

Eq. (6) is an integral equation of the 1st kind, this problem is ill-posed and requires regularization. Diminishing the coefficient α in (11), we can prevent highly oscillating solutions, therefore, this factor is really similar to a regularization parameter. The choice of the regularization parameter decides how well the solution fits the data. To find a suitable regularization parameter, we use the method of residuals (Lavrent'ev et al., 1986), which exploits information about data noise: we look for the smoothest possible solution, which field approximates the given data with the same accuracy as the data noise level.

Due to the fact that our approach to inversion is local, we could take a different value of the density contrast at each grid point. One should include a function of two variables $\Delta\sigma(x, y)$ into the integrand of Eq. (6), then use factors $\Delta\sigma_{ij} = \Delta\sigma(x_i, y_j)$ in the left hand of (7) and substitute the coefficient s in (11) by $s_{ij} = (G\Delta\sigma_{ij})^{-1}$. The same is valid for the depth to the asymptotic plane H . Sometimes it is reasonable, to divide the whole area into subareas and to use different values of H and $\Delta\sigma$ for each one. Within the method of local corrections it is also possible, which is demonstrated in the next section.

3 Gravity data inversion

A considerable amount of gravity data is now available to unravel the gross crustal structure of the Red Sea region. In order to investigate the structure of the northern Red Sea rift and Gulf of Suez, a new Bouguer gravity anomaly map has been prepared. It utilizes all available gravity data: Bouguer gravity data of the Egyptian General Petroleum Company published as a set of

Bouguer maps of Egypt at 1:500,000 scale in 1980; gravity surveys of the Gulf of Suez, Sinai and the Eastern Desert conducted by the Sahara Petroleum Company (SAPETCO) and PHILIPS Company between 1954 and 1958; marine gravity data in the northern Red Sea measured by the research vessel "Robert D. Conrad" to the north of 26° N in 1984. All the data of these surveys were compiled, classified and ranked according to instrument sensitivity and measurement density. More details on how the Bouguer map was compiled can be found in (Saleh et al., 2006). The resulting Bouguer map is shown in Fig. 1.

Fig. 1.

The calculated Bouguer gravity anomaly is reduced to sea level and corrected for mass effects of topography with the standard density of reduction 2670 kg/m^3 . The general trend of the Bouguer gravity anomalies is northwest-southeast. The anomaly increases in magnitude with a decrease in the relief of the topography and attains its maximum of $+95 \text{ mGal}$ along the axis of the Red Sea rift floor.

The main goal of our investigation is to extract the gravity signal from the Moho boundary and to find its 3D topography. At the first stage, we separate near-surface and deeper sources by means of the algorithm of upward and downward continuation described in section 2. Gravitational effects of shallow and deeper sources are shown in Fig. 2.

Fig. 2.

According to the obtained field of shallow sources a model of the horizontal layer above the depth of 7 km is found using the method of local corrections from section 2, which includes a generalized density interface between light sediments with a mean density value of 2300 kg/m^3 and crystalline basement with density of 2750 kg/m^3 . Its depressions and uplifts correspond to known geological structures. We present in Fig. 3 a position of the obtained contact surface along a profile 28° of northern latitude. Presented is a depression of the light material, then an uplift of dense rocks near Gebel El Zeit, a depression of the light (sedimentary) material below the Gulf of Suez, an uplift of dense material below Sinai Peninsula, a depression below the Gulf of Aqaba, then an uplift of dense rocks near the coast of Saudi Arabia.

Fig. 3.

At the next stage, we isolate the effect of very deep sources (below 100 km) and sources outside the area of investigation. We apply again the algorithm described in section 2. This time the part of the residual field has been found, which is harmonic above the depth of 100 km. A possible source of the positive anomaly could be an uplift of asthenosphere. After subtracting this field from

the total effect of deeper sources shown in Fig. 2, we obtain the contribution of the Moho interface. The gravitational signal from the half-space below 100 km and the effect of the Moho boundary are presented in Fig. 4.

Fig. 4.

Using the obtained residual field as a given data, we solve the inverse problem for a 3D topography of the Moho boundary. The method of local corrections is applied, which is described in section 2.

We make inversion separately for the area of rifts (Red Sea, Gulf of Suez and Gulf of Aqaba) and for the rest of the area. In the rift area we look for the upper boundary of the low-density, heated anomalous upper mantle with density of 3100 kg/m^3 . We assume that the ambient medium has a horizontally layered structure, it consists of the layer with density 2750 kg/m^3 above the depth of 20 km, the layer with density 2900 kg/m^3 between 20 and 30 km and the layer with density 3250 kg/m^3 below 30 km. If the upper boundary of the anomalous mantle intersects both mentioned layers, it has a density contrast with the ambient medium of 350 kg/m^3 above the depth of 20 km, 200 kg/m^3 between 20 and 30 km and -150 kg/m^3 below 30 km. The depth to the asymptotic plane H (see section 2) equals to 50 km. The found topography is shown in Fig. 5, the altitude above the depth of 30 km is presented, +17 km means the depth to the density interface of $30 - 17 = 13$ km, +2 km - the depth of $30 - 2 = 28$ km.

In the rest of the area the field is satisfied by means of a topography for the interface between material with density 2900 kg/m^3 (lower crust) and 3250 kg/m^3 (normal upper mantle). Density contrast amounts 350 kg/m^3 , the depth to the asymptotic plane is equal to 30 km. The obtained 3D topography is also presented in Fig. 5, again variations relative the depth of 30 km are shown.

Fig. 5.

We note that the density contrast $\Delta\sigma$ and the depth to the asymptotic plane H are different in different subareas and the ambient medium is not homogeneous in the vertical direction above and below the unknown contact surface, which is possible within the method of local corrections.

The amplitude of the residual field is less than 2 mGal. The main features of the obtained topography are quite in agreement with seismic information and results of previous gravity modeling (Saleh et al., 2006).

4 Magnetic data inversion

A new aeromagnetic map was compiled for both the Gulf of Suez and the northern Red Sea based on Cochran et al. (1986); Meshref (1990). The total magnetic intensity data resulting from different aeromagnetic surveys have been compiled and reduced to one set of data. The field has been reduced to the pole (Baranov, 1957), a regional magnetic effect has been subtracted (see Saleh et al. (2006)). Magnetic data is available for a smaller area, than in the gravitational case. The resulting total magnetic intensity data reduced to the pole is shown in Fig. 6.

Fig. 6.

We apply the algorithm of upward and downward continuation from section 2 to separate the effects of shallow and deeper sources. The Curie isotherms in the area are located above the depth of 15 km (Morgan et al., 1985), so we don't need to isolate the effect of very deep sources like in the gravitational case. The effect of deeper sources is attributed to variations of the Moho boundary topography. This effect, which we regard as a contribution of the Moho interface to the total field, is also presented in Fig. 6.

The model of the section is assumed, which consists of two layers: the upper one is magnetic and homogeneous (crust), the lower one is non-magnetic (heated anomalous upper mantle). An uplift of the non-magnetic mantle leads to magnetic crust thinning, which results in negative values of magnetic field.

If we put in Eq. (6) magnetization instead of density and apply the Poisson's relation (Blakely, 1995), we obtain an integral formula, which evaluates the magnetic field of the homogeneously magnetized layer contained between the surface with equation $z = z(x, y)$ and the plane $z = H$. This formula together with the fundamental equation to find the next approximation (9) provides the method of local corrections formula for the magnetic case analogous to (11).

Using the field of deeper sources shown in Fig. 6 as a given data, we solve the magnetic inverse problem for a 3D topography of the Moho boundary by means of the method of local corrections. The obtained topography is presented in Fig. 7. To make the magnetic model of the Moho topography comparable with the gravitational one, again the altitude above the depth of 30 km is presented; +17 km means the depth to the interface of $30 - 17 = 13$ km.

Fig. 7.

From our viewpoint, there are similarities between our gravitational and mag-

netic models of the Moho interface.

Both models agree well with the P-wave velocity distribution in the northern Red Sea and the Gulf of Suez (Gaulier et al., 1988). The gravitational model is also supported by refraction data in the areas not affected by the rifting event (Makris et al., 1983; El-Isa et al., 1987). The Moho topography magnetic model shows a poor flattening especially in the eastern region (e.g., Gaulier et al. (1988); Saleh et al. (2006)). The present results are in good agreement with the geothermal gradient values in the Red Sea (Cochran et al., 1986). The relatively low density of the anomalous upper mantle (3100 kg/m^3) of the Red Sea rift, as deduced from the gravity modeling, indicates the possible presence of partial melting in the upper mantle. The size of the area of anomalous upper mantle suggests that a large scale asthenospheric upwelling might be responsible for the subsequent rifting of the Red Sea. As a possible result of pressure release and convection heat, indicating a more advanced stage of rifting taking place in the northern part of Red Sea rift (which is interpreted as evidence for updoming due to the sea floor spreading in the central Red Sea), the crust becomes more oceanic in its nature. These results, which have been constrained by seismic measurements and confirmed by gravity and magnetic modeling, are in agreement with Cochran's concept of the northern part of the Red Sea (Cochran and Martinez, 1988; Saleh et al., 2006).

5 Summary and conclusions

Two new algorithms have been suggested to extract the signal from a contact surface and to find its 3D geometry. Both algorithms are applied to gravity and magnetic data for the area of the northern Red Sea including Gulf of Suez and Gulf of Aqaba to recover the Moho boundary topography. The following conclusions are drawn:

- (1) A new algorithm has been suggested to eliminate potential field sources from the Earth's surface to a prescribed depth h , based on upward and downward continuation. The solution of the 2D Dirichlet problem can be used as a model of the regional field. Subtracting the regional field from the observations prior to upward continuation allows integration of gravity data in the restricted area, while ignoring any information beyond the area of investigation. Downward continuation provides the part of the field, which is harmonic above the depth h . The properties of the integral operator give an opportunity to implement Lavrent'ev's regularization and to get rid of matrix multiplication. The algorithm has been successfully applied to separate the effects of shallow and deeper sources of gravity and magnetic field for the northern Red Sea area.
- (2) The method of local corrections is developed to recover 3D topography

of a contact surface. The method offers a simple and effective procedure for solving the nonlinear inverse problem without any linearization. This method does not make use of nonlinear minimization, which reduces the computer calculation time by an order of magnitude. We solve an integral equation for the function determining topography. We take into account instability of the inverse problem by means of a sort of regularization. The method of local corrections is applied for both gravity and magnetic data inversion to retrieve the 3D topography of the upper boundary of the heated anomalous mantle for the Red Sea rift area.

- (3) The gravitational and magnetic models of the Moho interface are obtained automatically without interactive forward modeling which dramatically diminishes the time expenditure. Both models are in agreement with seismic information and results of previous gravity modeling. There are similarities between the obtained gravitational and magnetic models of the Moho boundary. The uplift of the dense mantle and the thinning of the magnetic crust can explain low-frequency part of both gravity and magnetic field attributed to the Moho interface.

Acknowledgments

We would like to express our gratitude to the General Petroleum Company, Cairo, for utilizing the Bouger gravity data. Also, we would like to thank M. Hussain, Institute of Petroleum Research, for his encouragement and providing magnetic data.

References

- Baranov, W., 1957. A new method for interpretation of aeromagnetic maps: pseudo-gravimetric anomalies. *Geophysics* 22, 359–383.
- Blakely, R.J., 1995. *Potential Theory in Gravity and Magnetic Applications*. Cambridge University Press, Cambridge, 441 pp.
- Cochran, J.R., Martinez, F., Steckler, M.S., Hobart, M.A., 1986. Conrad deep: a new northern Red Sea deep. Origin and implications of continental rifting. *Earth Planet Sci. Lett.* 78, 18–32.
- Cochran, J.R., Martinez, F., 1988. Evidence from the northern Red Sea on the transition from continental to oceanic rifting. *Tectonophysics* 153, 25–53.
- Cordell, L., Henderson, R.G., 1968. Iterative three-dimensional solution of gravity anomaly data using a digital computer. *Geophysics* 33, 596–601.
- Drake, C.L., Girdler, R.W., 1964. A geophysical study of the Red Sea. *Geophys. J. R. Astron. Soc.* 8, 473–495.
- El-Isa, Z., Mechie, J., Prodehl, C., Makris, J., Rihm, R., 1987. A crustal struc-

- ture study of Jordan derived from seismic refraction data. *Tectonophysics* 138, 235–253.
- Gaulier, J.M., Le Pichon, X., Lyberis, N., Avedik, F., Geli, L., Moretti, I., Deschamps, A., Salah, H., 1988. Seismic study of the crust of the northern Red Sea and Gulf of Suez. *Tectonophysics* 153, 55–88.
- Gelfand, I.M., Fomin, S.V., 2000. *Calculus of Variations*. Dover Publications, New York, 240 pp.
- Gettings, M.E., Blank Jr., H.R., Mooney, W.D., Healy, J.H., 1986. Crustal structure of southwestern Saudi Arabia. *J. Geophys. Res.* 91(B6), 6491–6512.
- Ginzburg, A., Makris, J., Fuchs, K., Prodehl, C., 1981. The structure of the crust and upper mantle in the Dead Sea rift. *Tectonophysics* 80, 109–119.
- Götze, H.-J., Lahmeyer, B., 1988. Application of three-dimensional interactive modelling in gravity and magnetics. *Geophysics* 53, 1096–1108.
- Lavrent'ev, M.M., Romanov, V.G., Shishatskii, S.P., 1986. *Ill-Posed Problems of Mathematical Physics and Analysis*. Translations of Math. Monographs, v. 64, published by Amer. Math. Soc., Providence, 290 pp.
- Makris, J., Allam, A., Moktar, T., Basahel, A., Dehghani, G.A., Bazari, M., 1983. Crustal structure at the northwestern region of the Arabian shield and its transition to the Red Sea. *Bull. Fac. Earth Sci. K. Abdulaziz Univ.* 6, 435–447.
- Makris, J., Henke, C.H., Egloff, F., Akamaluk, T., 1991. The gravity field of the Red Sea and East Africa. *Tectonophysics* 198, 369–381.
- Martyshko, P.S., Prutkin, I.L., 2003. Technology of depth distribution of gravity field sources. *Geophys. J.* 25 (3), 159–168. (In Russian).
- Meshref, W.M., 1990. Tectonic framework. In: Said, R. (Ed.), *The geology of Egypt*. A.A. Balkema, Rotterdam, p.p. 113–155.
- Morgan, P., Boulos, F.K., Hennin, S.F., El-Sherif, A.A., El Sayed, A.A., Basta, N.Z., Melek, Y.S., 1985. Heat flow in Eastern Egypt: the thermal signature of continental breakup. *J. Geodyn.* 4, 107–131.
- Oldenburg, D., 1974. The inversion and interpretation of gravity anomalies. *Geophysics* 39, 526–536.
- Parker, R., 1972. The rapid calculation of potential anomalies. *Geophysical Journal of the Royal Astronomical Society* 31, 447–455.
- Prutkin, I.L., 1983. Approximate solution of three-dimensional gravimetric and magnetometric inverse problems by the method of local corrections. *Izvestiya. Physics of the Solid Earth* 19 (1), 38–41.
- Prutkin, I.L., 1986. The solution of three-dimensional inverse gravimetric problem in the class of contact surfaces by the method of local corrections. *Izvestiya. Physics of the Solid Earth* 22 (1), 49–55.
- Rihm, R., Makris, J., Moller, L., 1991. Seismic survey in the northern Red Sea: asymmetric crustal structure. *Tectonophysics* 198, 279–295.
- Saleh, S., Jahr, T., Jentzsch, G., Saleh, A., Abou Ashour, N.M., 2006. Crustal evaluation of the northern Red Sea rift and Gulf of Suez, Egypt from geophysical data: 3-dimensional modeling. *J. African Earth Sci.* 45, 257–278.

- Snopek, K., Casten, U., 2006. 3GRAINS: 3D Gravity Interpretation Software and its application to density modeling of the Hellenic subduction zone. *Computers & Geosciences* 32 (5), 592–603.
- Tirel, C., Gueydan, F., Tiberi, C., Brun, J.-P., 2004. Aegean crustal thickness inferred from gravity inversion. Geodynamical implications. *Earth and Planetary Science Letters* 228, 267–280.
- Tramontini, C., Davies, D., 1969. A seismic refraction survey in the Red Sea. *Geophys. J. R. Astron. Soc.* 17, 2225–2241.
- Vasin, V.V., Prutkin, I.L., Timerkhanova, L.Yu., 1996. Retrieval of a Three-Dimensional Relief of Geological Boundary from Gravity Data. *Izvestiya. Physics of the Solid Earth* 32 (11), 901–905.

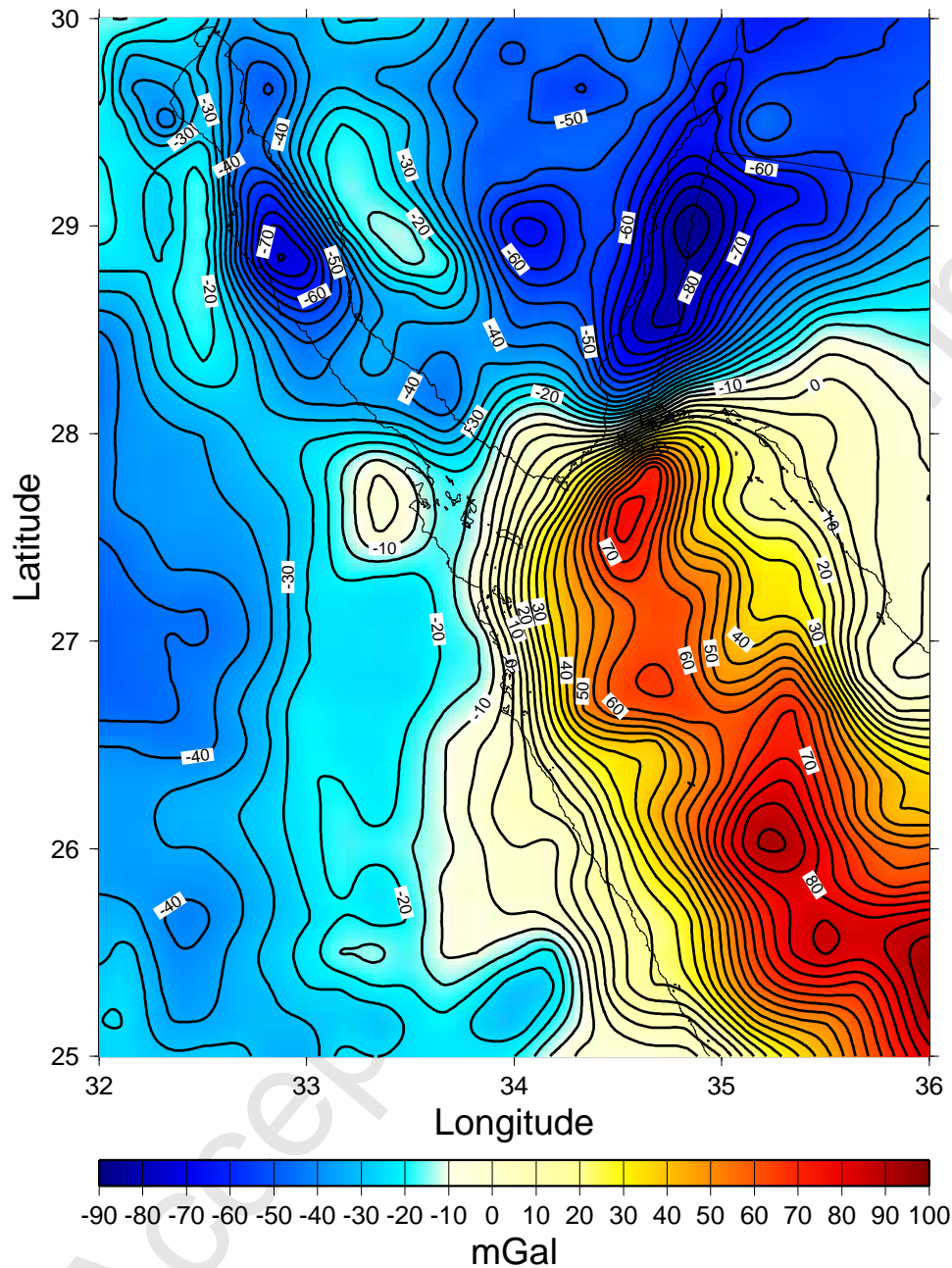


Fig. 1. Bouguer gravity anomaly for Red Sea and surrounding region. Contour interval is 10 mGal. Data are corrected for mass effects of topography using reduction density of 2670 kg/m^3 .

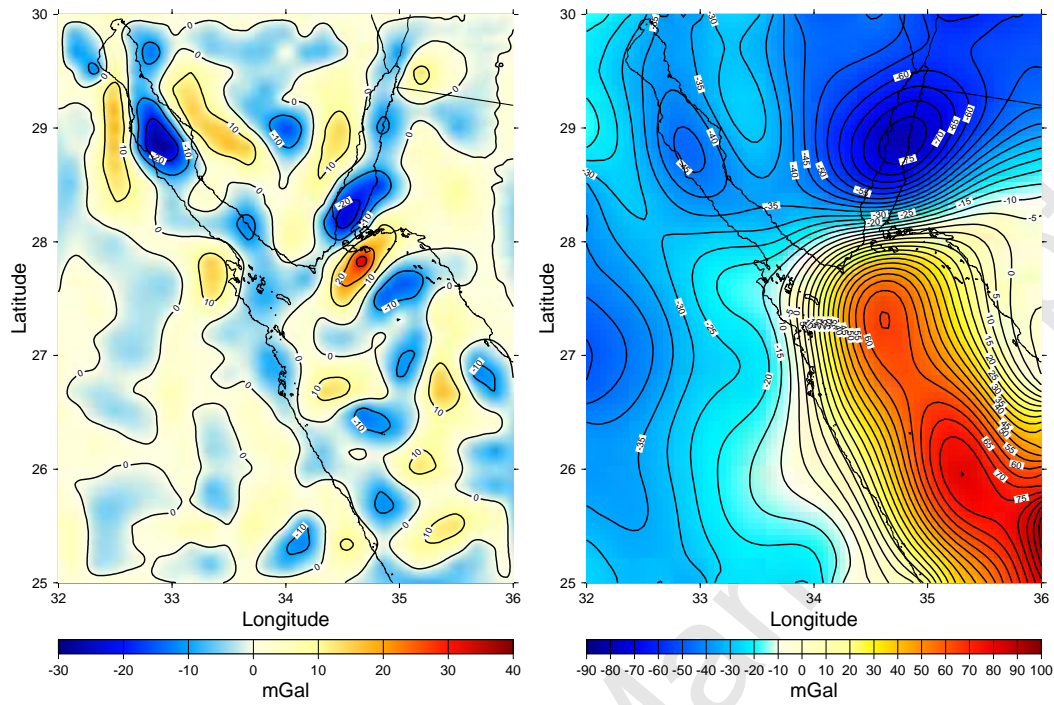


Fig. 2. Gravitational effects of shallow (left) and deeper (right) sources separated by means of algorithm of upward and downward continuation from section 2.

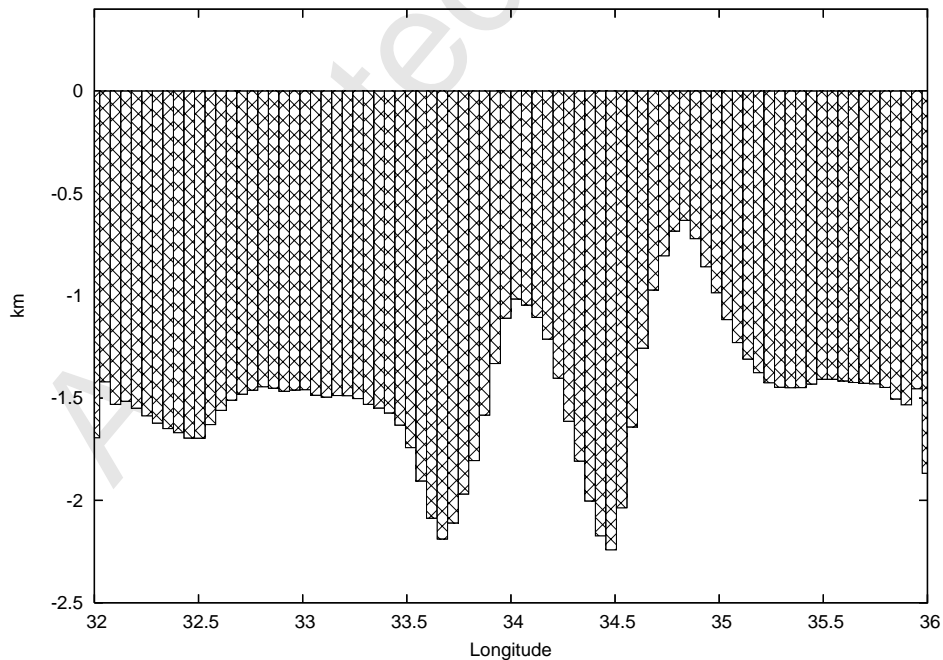


Fig. 3. Position of generalized density interface between light sediments with mean density value of 2300 kg/m^3 and crystalline basement with density of 2750 kg/m^3 along profile 28° N .

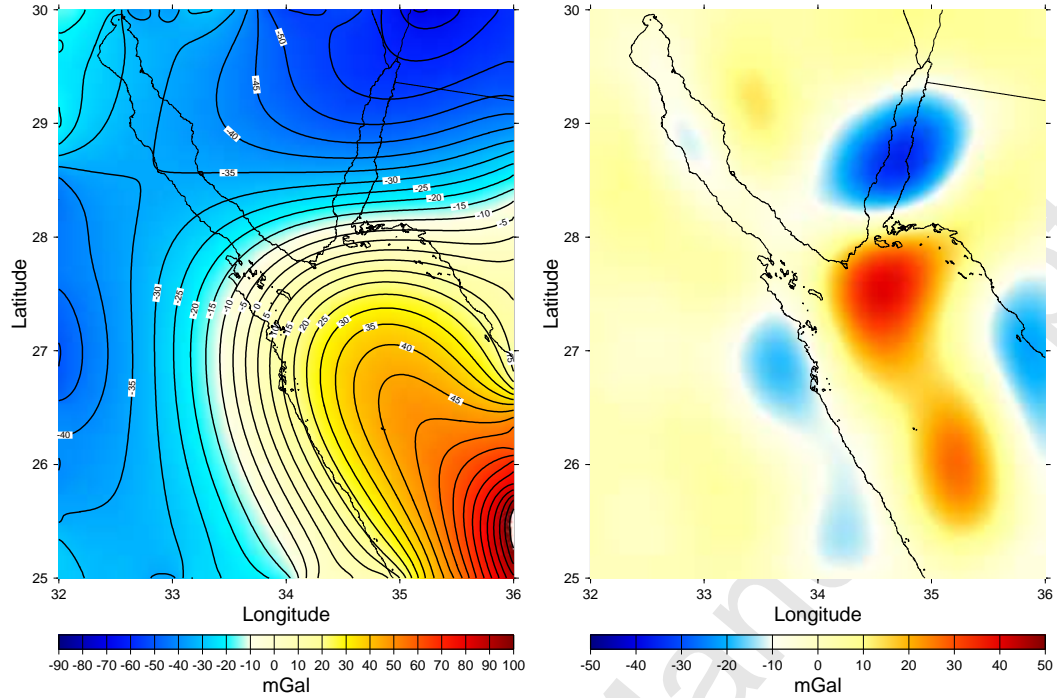


Fig. 4. Gravitational effects of very deep sources (below 100 km) and sources outside area of investigation (left) and contribution of Moho interface (right).

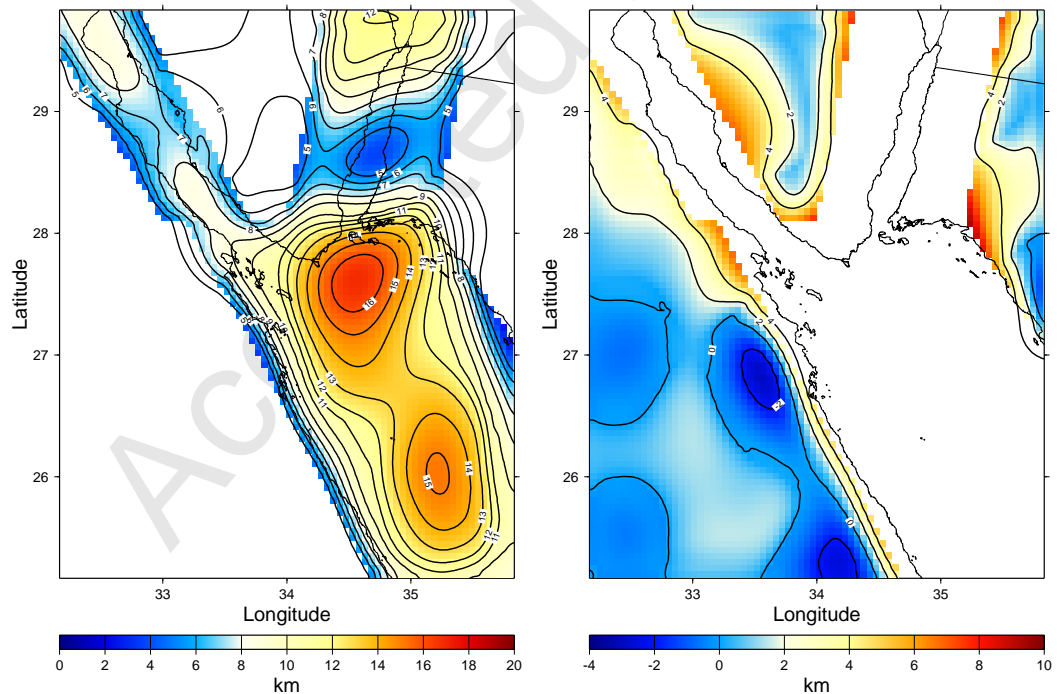


Fig. 5. Gravitational model of Moho topography within rift area (left) and for rest of region (right). It represents upper boundary of heated anomalous mantle with density 3100 kg/m^3 for rift area and interface between lower crust (density 2900 kg/m^3) and normal upper mantle (density 3250 kg/m^3) for rest of region.

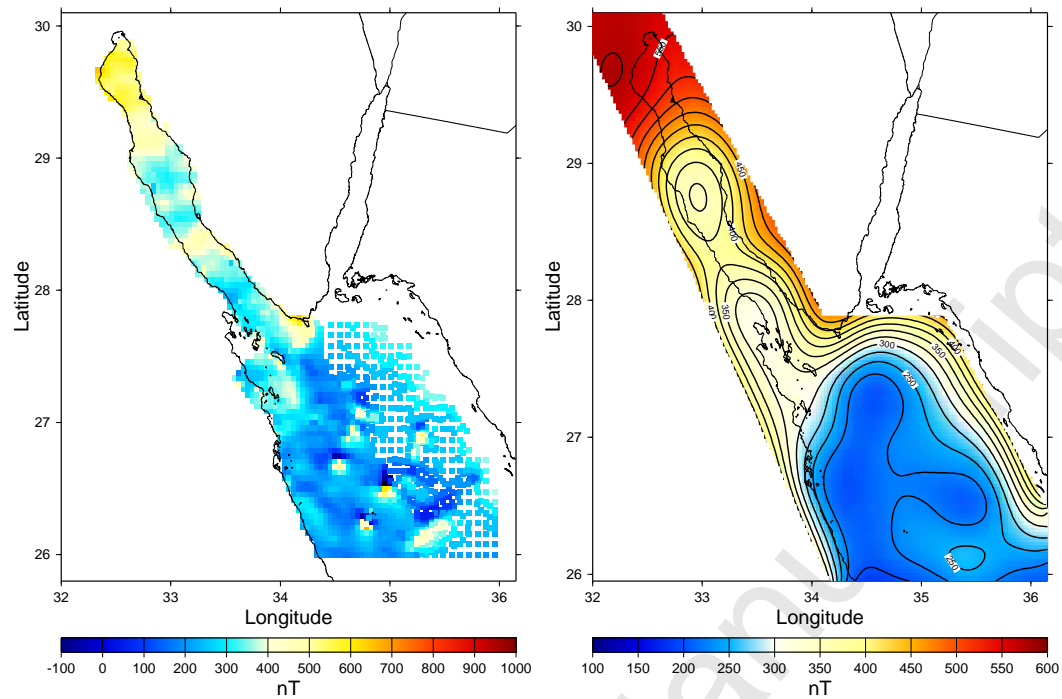


Fig. 6. Total magnetic intensity data reduced to pole (left) and magnetic field of deeper sources (right) obtained using algorithm of upward and downward continuation.

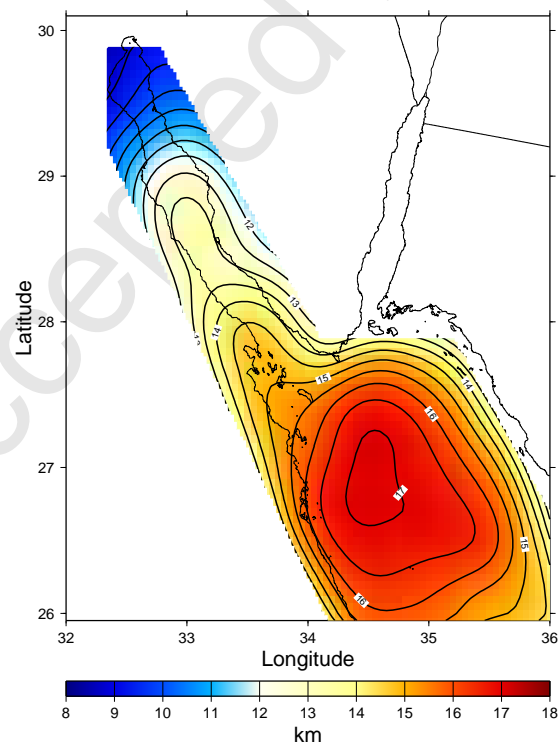


Fig. 7. Magnetic model of the Moho topography. It is obtained using method of local corrections from section 2 and represents interface between magnetic crust and non-magnetic anomalous upper mantle.